

Optimization algorithms for steady state analysis of self excited induction generator

Ibrahim Athamnah¹, Yaser Anagreh¹, Aysha Anagreh²

¹Electrical Power Engineering Department, Hijjawi Faculty for Engineering Technology, Yarmouk University, Irbid, Jordan

²Department of Educational Sciences, Faculty of Irbid College, AlBalqa Applied University, As-Salt, Jordan

Article Info

Article history:

Received Jul 23, 2022

Revised Jul 2, 2023

Accepted Jul 4, 2023

Keywords:

Genetic algorithm

Grey wolf optimization

MATLAB optimizers

Particle swarm optimization

Whale optimization algorithm

ABSTRACT

The current publication is directed to evaluate the steady state performance of three-phase self-excited induction generator (SEIG) utilizing particle swarm optimization (PSO), grey wolf optimization (GWO), wale optimization algorithm (WOA), genetic algorithm (GA), and three MATLAB optimization functions (*fminimax*, *fmincon*, *fminunc*). The behavior of the output voltage and frequency under a vast range of variation in the load, rotational speed and excitation capacitance is examined for each optimizer. A comparison made shows that the most accurate results are obtained with GA followed by GWO. Consequently, GA optimizer can be categorized as the best choice to analyze the generator under various conditions.

This is an open access article under the [CC BY-SA](https://creativecommons.org/licenses/by-sa/4.0/) license.



Corresponding Author:

Yaser Anagreh

Electrical Power Engineering Department, Hijjawi Faculty for Engineering Technology, Yarmouk University
Irbid, Jordan

Email: anagrehy@yu.edu.jo

1. INTRODUCTION

Nowadays induction generators are extensively used in renewable energy systems, especially hydro and wind-based energy systems. This is due to a number of advantages of this generator type including low cost, simple construction, ease of maintenance and natural protection against short circuits [1]. To supply electrical loads in remote rural areas, where the network is far away, standalone induction generator is the most attractive choice [2]. An induction machine can be operated as a self-excited induction generator (SEIG) due to the presence of residual flux in the stator and rotor cores. If the generator is driven at a suitable speed and appropriate excitation capacitors are connected across the stator terminals, the voltage is built up until saturation region is attained [3]. In the literature, a great number of publications have been directed to evaluate the steady state performance of SEIG using various optimization techniques.

Nigim *et al.* [4] have implemented MathCad software package to estimate the unknown parameters of SEIG, which is operated in the saturation region to achieve better performance. Singaravelu and Velusami [5] have used fuzzy logic approach to find the unknown variables of SEIG under steady state operation. Mahato *et al.* [6] have avoided the solution of high order polynomial by using the eigen value sensitivity technique to determine the excitation capacitance limits in achieving high SEIG performance under steady state operation. Haque [7] have utilized *fsolve* algorithm, which is built in MATLAB, to analyze different configurations of SEIG. They found that short shunt SEIG type has possessed the best steady state performance, compared with shunt and long shunt schemes. Kheldoun *et al.* [8] have implemented the DIRECT algorithm to find the frequency and magnetizing reactance by minimizing the total admittance of the SEIG equivalent circuit. In this algorithm, an initial guess for the unknowns is not needed, only their boundaries are required.

Hasanien and Hashem [9] have used cuckoo search algorithm (CSA) to minimize the total impedance equation of wind driven SEIG and assess the steady state performance of the generator. Boora *et al.* [10] have used the concept of symmetrical components with the fsolve algorithm to find the unknown parameters of a capacitive excited induction generator (CEIG) under unbalanced operating conditions. Saha and Sandhu [11] have made a comparison for the implementation of genetic algorithm (GA), particle swarm optimization (PSO) and simulated annealing (SA) algorithm for predicting the steady state performance of SEIG feeding balanced resistive load.

In the present research work PSO, grey wolf optimization (GWO), wale optimization algorithm (WOA), GA and three MATLAB optimization functions (*fminimax*, *fmincon*, *fminunc*) are utilized for minimizing the total impedance equation of SEIG circuit model in order to find the two unknown parameters F and X_m . The behaviors of the voltage and frequency when applying changes in the load impedance, speed or excitation capacitance are examined for each algorithm. The same operating conditions are considered when applying the optimization approaches, and based on the obtained results a comparison is made. The generator's steady state model is derived from its dynamic direct quadrature (DQ) representation.

2. MATHEMATICAL MODELING

The DQ steady state (SS) model of a SEIG can be derived by setting the time derivative of the DQ dynamic model to zero [12]. The SS model can be given in (1) to (4):

$$v_{qs} = r_s i_{qs} + \omega_e (L_s i_{ds} + L_m i_{dr}) \quad (1)$$

$$v_{ds} = r_s i_{ds} + \omega_e (L_s i_{qs} + L_m i_{qr}) \quad (2)$$

$$v_{qr} = r_r i_{qr} + (\omega_e - \omega_r) (L_r i_{dr} + L_m i_{ds}) \quad (3)$$

$$v_{dr} = r_r i_{dr} - (\omega_e - \omega_r) (L_r i_{qr} + L_m i_{qs}) \quad (4)$$

where $L_s = L_{ls} + L_m$ and $L_r = L_{lr} + L_m$, L_{ls} and L_{lr} are the leakage inductances of stator and rotor winding; L_m is the mutual inductance; r_s and r_r are stator resistance and rotor resistance; v_{qs} and v_{ds} are qd -stator voltages; v_{qr} and v_{dr} are qd -rotor voltages; i_{qs} , i_{ds} are dq -stator currents; i_{qr} and i_{dr} are qd -rotor currents; ω_e and ω_r are the synchronous and rotor speeds. Equations (1) to (4) can be rewritten in terms of the complex rms space voltage vectors as (5) and (6).

$$\vec{V}_{qs} - j\vec{V}_{ds} = (r_s + j\omega_e L_s)(\vec{I}_{qs} - j\vec{I}_{ds}) + j\omega_e L_m(\vec{I}_{qr} - j\vec{I}_{dr}) \quad (5)$$

$$\vec{V}_{qr} - j\vec{V}_{dr} = j(\omega_e - \omega_r)L_m(\vec{I}_{qs} - j\vec{I}_{ds}) + [r_r + j(\omega_e - \omega_r)L_r](\vec{I}_{qr} - j\vec{I}_{dr}) \quad (6)$$

Using the relationships between the rms space vectors and rms time phasors, rewriting the slip frequency ($\omega_e - \omega_r$) by the slip multiplied by synchronous speed ($s\omega_e$), and dropping the common $e^{j\omega t}$ term yields (7) and (8) [12].

$$\vec{V}_s = (r_s + j\omega_e L_{ls})\vec{I}_s + j\omega_e L_m(\vec{I}_s + \vec{I}_r) \quad (7)$$

$$\vec{V}_r = (r_r + js\omega_e L_{lr})\vec{I}_r + js\omega_e L_m(\vec{I}_s + \vec{I}_r) \quad (8)$$

Divide the last equation by the per unit slip s yields (9).

$$\frac{\vec{V}_r}{s} = \left(\frac{r_r}{s} + j\omega_e L_{lr} \right) \vec{I}_r + j\omega_e L_m(\vec{I}_s + \vec{I}_r) \quad (9)$$

The slip s can be expressed as (10).

$$s = \frac{\omega_e - \omega_r}{\omega_e} = \frac{\frac{f}{f_b} - \frac{\omega_r}{2\pi f_b}}{\frac{f}{f_b}} = \frac{F - u}{F} \quad (10)$$

where F is the ratio of the actual frequency to base frequency and u is the ratio of the running speed to the synchronous speed, which corresponds to the base frequency. Since SEIG could be driven at different speeds and accordingly variable stator frequency, it is convenient to refer all of the machine parameters to rated frequency. The per unit steady state equivalent circuit of the SEIG feeding RL-load is shown in Figure 1 [13]. All of the circuit parameters, except X_m , are postulated fixed and not affected by magnetic saturation [7]–[9]. Application of Kirchhoff's voltage law (KVL) to the circuit model of SEIG providing that the equivalent Thevenin impedance must equal to zero, since the current $I_s \neq 0$ [14]:

$$Z_{total} = Z_s + (Z_C // Z_L) + (Z_r // Z_m) = 0 \tag{11}$$

where $Z_s = \frac{R_s}{F} + j X_s, \quad Z_C = -j \frac{X_C}{F^2}, \quad Z_L = \frac{R_L}{F} + j X_L,$
 $Z_r = \frac{R_r}{F-u} + j X_r, \quad Z_m = j X_m$

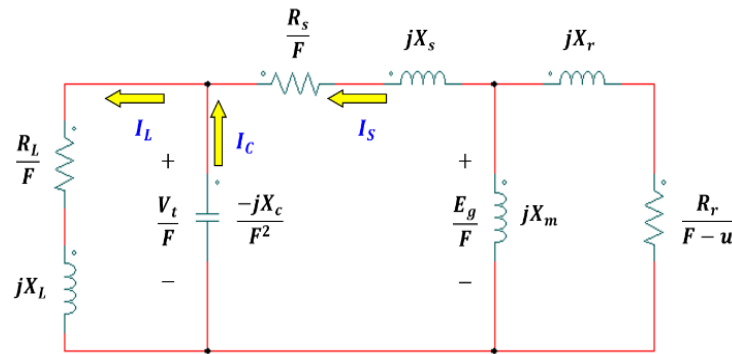


Figure 1. The per unit steady state model of SEIG

3. OPTIMIZATION ALGORITHMS

To achieve numerical solution for the total impedance equation of SEIG, it is required to formulate the equation as an objective function [14], which is given in (12). An optimization algorithm could be used to solve this equation and find the two unknown parameters under different operating conditions. The performance of the SEIG can be evaluated using the obtained values of the unknown parameters, with the help of the generator equivalent circuit. In the current research work several optimization techniques are utilized to find the two unknown parameters X_m and F . The main concepts for each of these techniques are presented in the following sub-sections.

$$\begin{aligned} &Min[Z_{total}(F, X_m)] \\ &Subject\ to\ the\ constraints \begin{cases} 0.5 \leq F \leq 1.0 \\ 0.2 \leq X_m \leq 2.25 \end{cases} \end{aligned} \tag{12}$$

3.1. Particle swarm optimization

PSO is involved in several iterations of updating both the position and velocity of each particle in the swarm to achieve the best solution, with respect to a certain quality measure [15]. Figure 2 presents the algorithm's flowchart. The position and velocity of a particle in the swarm can be mathematically represented in the (13) and (14) [16], [17]:

$$V_j^{(K+1)} = \mu V_j^K + \delta_1 rand[0,1](P_{best} - X_j^K) + \delta_2 rand[0,1](G_{best} - X_j^K) \tag{13}$$

$$X_j^{(K+1)} = X_j^K + V_j^{(K+1)} \tag{14}$$

where $V_j^{(K+1)}$ is the particle speed, $X_j^{(K+1)}$ is th particle position, u is the inertia of the particle, δ_1 and δ_2 are positive constants, P_{best} is the best solution for the particle and G_{best} is the best position of the swarm. Using the objective function $f(F, X_m)$, P_{best} and G_{best} can be defined in (15)-(16):

$$P_{best}^{(K+1)} = \begin{cases} P_{best}^{(K)}, & X_j^{(K+1)} \geq f(P_{best}^{(K)}) \\ X_j^{(K+1)}, & X_j^{(K+1)} < f(P_{best}^{(K)}) \end{cases} \quad (15)$$

$$G_{best}^{(K)} = \text{argmin}_{i=1}^n \{f(P_{best}^{(K)})\} \quad (16)$$

where $f(P_{best}^{(K)})$ is the K^{th} value of our objective function $f(F, X_m)$ and n is the total number of particles [18], [19].

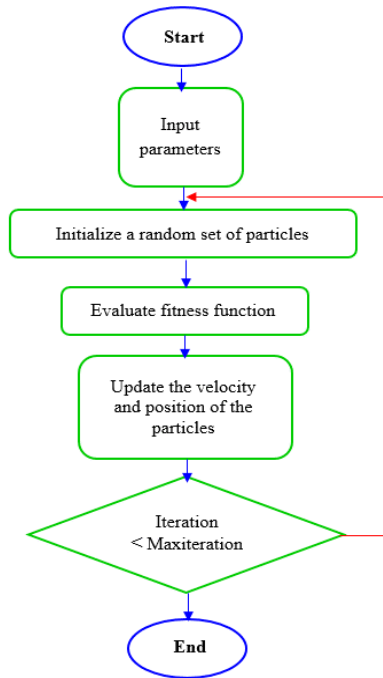


Figure 2. Flowchart of PSO algorithm

3.2. Grey wolf optimization algorithm

The implementation of GWO is performed based on the hunting mechanism of grey wolves: alpha, beta, delta, and omega [20]–[22]. The mathematical representation of GWO is given in (17) to (20) [23]:

$$D = |C \times X_p(q) - X(q)| \quad (17)$$

$$X(q+1) = X_p(q) - A \times D \quad (18)$$

$$C = 2 \times r_2 \quad (19)$$

$$A = a \times (2 \times r_1 - 1) \quad (20)$$

where D is the distance of the wolf, q is the iteration, X_p is the prey position, X is the wolf location, C , A and a are coefficients, r_1 and r_2 are random vectors. The objective function $f(F, X_m)$ can be mathematically formulated based on GWO algorithm, as given in (21) to (23). The unknowns X_m and F are called and compared with the wolf locations (X_α , X_β , X_δ), and these locations are then updated to reach the final best solution.

$$\text{If } \{f(F, X_m) < X_\alpha \quad \text{then } X_\alpha = f(F, X_m)\} \quad (21)$$

$$\text{If } \left\{ \begin{array}{l} f(F, X_m) > X_\alpha \\ f(F, X_m) < X_\beta \end{array} \right. \quad \text{then } X_\beta = f(F, X_m) \quad (22)$$

$$\text{If } \left\{ \begin{array}{l} f(F, X_m) > X_\alpha \\ f(F, X_m) > X_\beta \text{ then } X_\delta = f(F, X_m) \\ f(F, X_m) < X_\delta \end{array} \right\} \quad (23)$$

The distances as well as locations of wolfs can be recalculated and updated based on the (24) to (29).

$$D_\alpha = |C_1 \times X_\alpha - X(q)| \quad (24)$$

$$D_\beta = |C_2 \times X_\beta - X(q)| \quad (25)$$

$$D_\delta = |C_3 \times X_\delta - X(q)| \quad (26)$$

$$X_1 = |X_\alpha - a_1 D_\alpha| \quad (27)$$

$$X_2 = |X_\beta - a_2 D_\beta| \quad (28)$$

$$X_3 = |X_\delta - a_3 D_\delta| \quad (29)$$

The new position of the prey, which depends on the locations and distances of the three main wolfs, can be recalculated and updated based on the (30) [23].

$$X_p(q+1) = \frac{X_1 + X_2 + X_3}{3} \quad (30)$$

3.3. MATLAB based algorithms

The three algorithms *fminimax*, *fmincon*, and *fminunc* are built in MATLAB optimization toolbox. The operation of *fminimax* optimizer is based on Newton optimization approach [24]. It minimizes the worst-case value for a set of multivariable functions, starting at an initial estimate. Since the objective function $f(F, X_m)$ is differentiable and the aim is to approach $f(F, X_m) = F(X) = 0$, it is possible to solve the equation by letting X_0 , as an initial point, and expressing the current value of an unknown variable in the (31).

$$X_{n+1} = X_n - \frac{F'(X_n)}{F(X_n)} \quad n = 0, 1, \dots \text{ etc} \quad (31)$$

fmincon can find a constrained minimum of a scalar function of several variables starting at an initial estimate. It is usually applied to solve medium and large scale optimization problems [25]. The use of *fmincon* function to minimize the total impedance equation can be represented as (32).

$$\min_x f(F, X_m) \text{ such that } \left\{ \begin{array}{l} C(x) \leq 0 \\ Ceq(x) = 0 \\ A \cdot x \leq b \\ Aeq \cdot x = beq \\ lb \leq x \leq ub \end{array} \right\} \quad (32)$$

fminunc could be used to find an unconstrained minimum of a scalar function having several variables starting at an initial estimate [26]. It is similar to *fmincon* in the way of its utilization for the objective function $f(F, X_m)$, but the iterations are not bounded with any constraint.

3.4. Whale optimization algorithm

WOA is based on humpback whales hunting method, which involves in shrinking encircling mechanism and spiral updating position. It starts with a set of random solutions followed by iterations trying to find the best solution. The search agents are updated their locations based on either a randomly selected search agent or the best obtained solution in the prior iteration [27]. The method of WOA can be formulated in (33) and (34) [14], [28]:

$$\vec{D} = |\vec{C} \vec{X}^*(t) - \vec{X}(t)| \quad (33)$$

$$\vec{X}(t+1) = \begin{cases} \vec{X}^*(t) - \vec{A} \cdot \vec{D} & \text{if } p < 0.5 \\ \vec{D} \cdot e^{bl} \cos(2\pi l) + \vec{X}^*(t) & \text{if } p \geq 0.5 \end{cases} \quad (34)$$

where t is the present iteration, \vec{X} is the position vector, \vec{X}^* is the position vector of the obtained best solution of the present iteration and is updated at each iteration, p is a random number in the interval of $[0,1]$, l is a random number in the interval of $[-1,1]$, b is a constant. The coefficient vectors \vec{A} and \vec{C} can be expressed in (35) and (36).

$$\vec{A} = 2\vec{a} \cdot \vec{r} - \vec{a} \quad (35)$$

$$\vec{C} = 2 \cdot \vec{r} \quad (36)$$

where \vec{r} is a random vector, \vec{a} is located between 2 and 0. The unknown variables of the objective function $f(F, X_m)$ are called and compared with the values of the whale leader vector position \vec{X} . The values of the vector are updated, if the comparison for the obtained result does not satisfy the preset criteria. The comparison can be mathematically represented as (37).

$$\text{If } \{f(F, X_m) < \vec{X} \quad \text{then } \vec{X} = f(F, X_m) \quad (37)$$

3.5. Genetic algorithm

The process of GA optimization is started with initial population depending on the formulated chromosomes, which represent the unknown variables of the problem. The population which is also called generation provides a set of possible solutions. To reach the best solution, the population is subjected to repetitive iterations for selection crossover, mutation and inversion. The GA optimization process flowchart is presented in Figure 3.

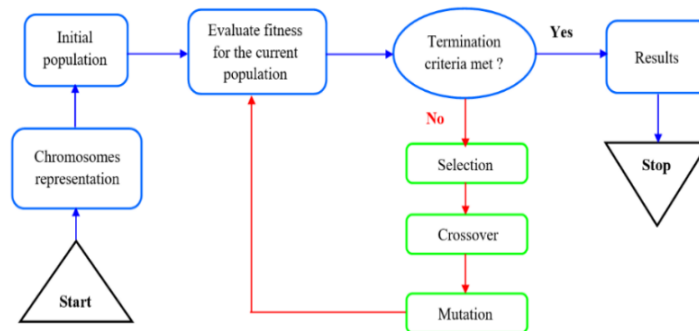


Figure 3. The process of GA optimization

In the present work, the parameters of each individual (chromosome) represent the unknown parameters X_m and F ; chromosome = $[X_m F]$. If Pop is the total number of the population then the crossover process is reiterated by $(\text{Pop}/2)$ times, and moreover another Pop children will be produced [29]. If parents are $[X_{m1} F_1]$ and $[X_{m2} F_2]$ then:

$$\text{Child} - 1 = \begin{cases} X_m = rX_{m1} + (1-r)X_{m2} \\ F = rF_1 + (1-r)F_2 \end{cases} \quad (38)$$

$$\text{Child} - 2 = \begin{cases} X_m = (1-r)X_{m1} + rX_{m2} \\ F = (1-r)F_1 + rF_2 \end{cases} \quad (39)$$

where r is the crossover rate, which is selected randomly between 0 and 1, and is selected to be 0.9. High value of crossover rate is selected to preserve genetic information for each individual and moreover maintaining acceptable behavior for the crossover process. To prevent local optima premature convergence, mutation process is applied. Equations (40) and (41) describe the mutation operator for real valued encoding.

$$X_m = X_m + (r_1 - 0.5)(2 X_{m_max}) \quad (40)$$

$$F = F + (r_2 - 0.5)(2 F_{max}) \quad (41)$$

where X_m and F are the parameters in each child, X_{m_max} and F_{max} are the maximum variations in the variables X_m and F when applying the mutation process, r_1 and r_2 are two random numbers representing the mutation rate; $r_1, r_2 \in (0, 1)$.

4. RESULTS AND DISCUSSION

The machine used in the current investigation is 1.5 kW 380 V 3.7 A 50 Hz 1,415 r.p.m 4-pole 0.77 PF lagging Y-connected three-phase squirrel cage induction generator. The per unit values of stator resistance, rotor resistance, stator reactance, rotor reactance and saturated magnetizing reactance are 0.07, 0.16, 0.22, 0.34 and 2.25, respectively. The nonlinear relation between E_g/F and X_m is given by:

$$\frac{E_g}{F} = -0.46 X_m^3 + 1.32 X_m^2 - 1.31 X_m + 1.54.$$

To assess the implementation of the considered optimization techniques for steady state analysis of SEIG, the behavior of the output voltage (V_o) and output frequency (F) under the variations in the load impedance (Z_L), rotational speed (u) or excitation capacitance (C) are examined. The considered ranges in varying these three parameters are given in Table 1. To achieve fair comparison for the utilized optimization approaches, extensive MATLAB/Simulink simulations under the same operating conditions for all approaches are conducted. The obtained results for each algorithm are presented in this section.

Table 1. The ranges in varying SEIG parameters during simulation

Case No.	Range	Z_L (p.u.)	u (p.u.)	C (μ F)
1	2.2-10	variable	1.0	120
2	0.8-1.6	2.2	variable	120
3	50-220	2.2	1.0	variable

The results of utilizing the PSO algorithm to examine the behavior of the obtained voltage (V_o) and frequency (F) when varying the load impedance (Z_L), speed (u) and excitation capacitance (C) are presented in Figure 4: the behavior of V_o and F versus Z_L is shown in Figure 4(a), the variation of V_o and F versus u is presented in Figures 4(b) and 4(c) demonstrates the changes of V_o and F against C . It can be clearly noticed that the PSO algorithm fails to find the optimum unknown values at some values of the load impedance and speed. Figure 5 shows the obtained results for the voltage and frequency when implementing GWO algorithm under the same operating conditions. Figure 5(a) shows the behavior of V_o and F versus Z_L , the variation of V_o and F versus u is presented in Figure 5(b) and the behavior of V_o and F against C is demonstrated in Figure 5(c). It can be observed that GWO is succeeded in finding the unknown variables F and X_m for the whole considered ranges of variations in Z_L , u or C . As a result, acceptable curves representing the behavior of V_o and F are acquired. Comparing the GWO results with the corresponding PSO results, tremendous improvement is achieved when using GWO algorithm.

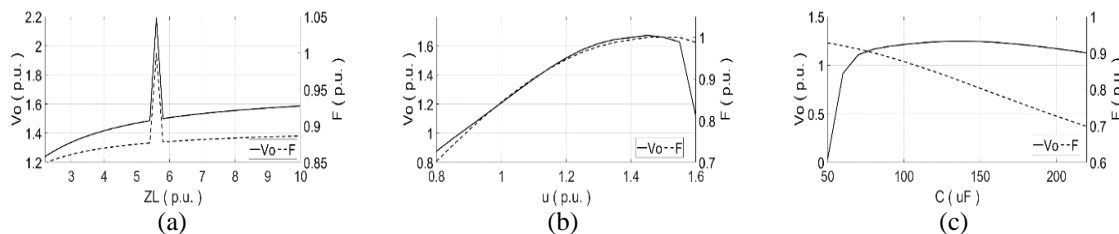


Figure 4. The results of PSO algorithm for the obtained voltage and frequency versus the load, speed or the excitation capacitance (a) V_o and F versus Z_L , (b) V_o and F versus u , and (c) V_o and F versus C

The obtained results when using MATLAB built in algorithms *fminimax*, *fmincon* and *fminunc*, under the same considerations for PSO and GWO algorithms, are presented in Figures 6 to 8, respectively. The variations of V_o and F with Z_L , their variations with u and the behavior of these two outputs versus C , when utilizing *fminimax* algorithm, are shown in Figures 6(a), 6(b) and 6(c), respectively. The results of *fmincon* algorithm that demonstrating the behavior of V_o and F against the changes in Z_L , u and C are presented in

Figures 7(a), 7(b), and 7(c), respectively. The changes of the two outputs; V_o and F , versus Z_L , u and C , when implementing *fminunc*, are shown in Figures 8(a), 8(b), and 8(c), respectively. It can be seen that *fminimax* and *fmincon* algorithms fail to find the optimum unknown values below 1 per unit speed. Therefore, these two algorithms are not appropriate to be used under low-speed operation. From the results in Figure 8, it can be noticed that *fminunc* is unable to find the optimum unknown values under the variations in the load impedance or rotational speed.

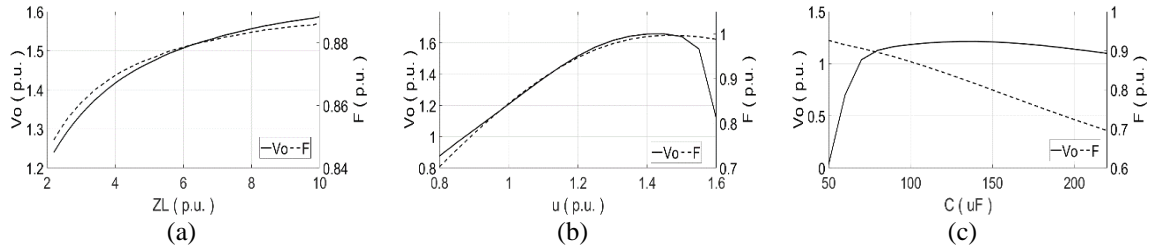


Figure 5. The results of GWO algorithm for the obtained voltage and frequency against the load, speed or the excitation capacitance (a) V_o and F versus Z_L , (b) V_o and F versus u , and (c) V_o and F versus C

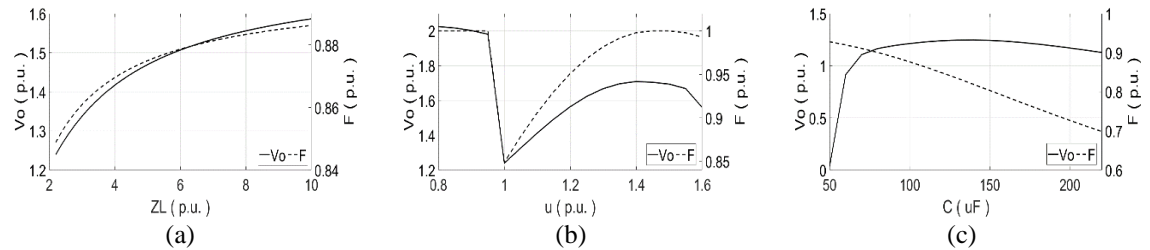


Figure 6. The results of *fminimax* algorithm for the obtained voltage and frequency against the load, speed or the excitation capacitance (a) V_o and F versus Z_L , (b) V_o and F versus u , and (c) V_o and F versus C

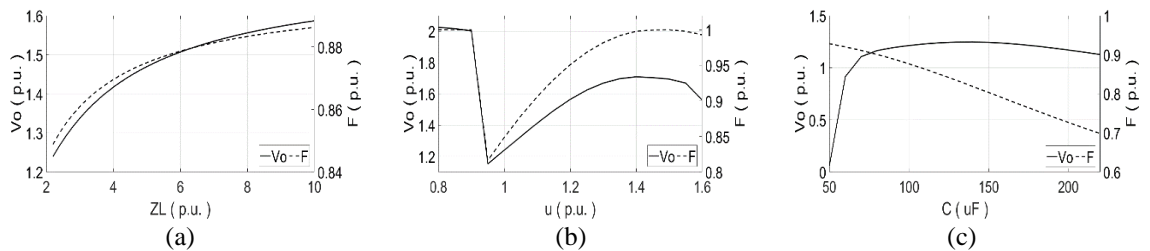


Figure 7. The results of *fmincon* algorithm for the obtained voltage and frequency against the load, speed or the excitation capacitance (a) V_o and F versus Z_L , (b) V_o and F versus u , and (c) V_o and F versus C

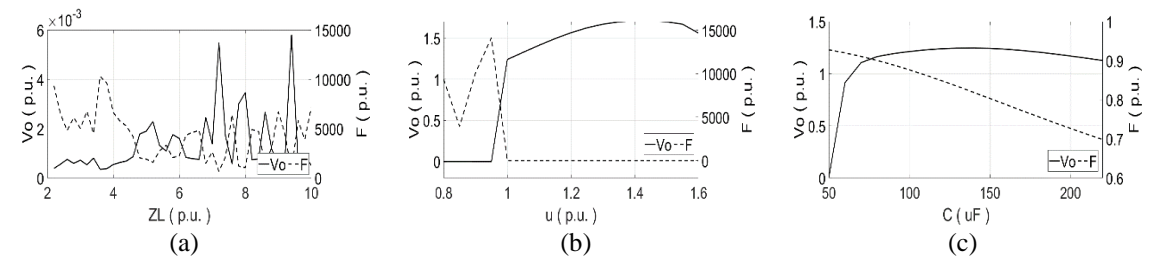


Figure 8. The results of *fminunc* algorithm for the obtained voltage and frequency against the load, speed or the excitation capacitance (a) V_o and F versus Z_L , (b) V_o and F versus u , and (c) V_o and F versus C

The results of the output voltage and frequency against load impedance, speed and excitation capacitance using WOA algorithm are presented in Figure 9. The behavior of V_o and F versus Z_L is shown in Figure 9(a), the variation of V_o and F versus u is presented in Figures 9(b) and 9(c) demonstrates the changes of V_o and F against C . It can be noticed that WOA algorithm fails to find accurate unknown values for load impedance greater than 3 per unit, and moreover inaccurate results are obtained for excitation capacitance above 125 μF . In addition, the algorithm could not find the optimum unknown values below 1 pu speed. The weakness in the accuracy of the obtained results for the unknown variables is reflected in the smoothness of the curves representing V_o and F results.

Figures 10 presents the results of genetic algorithm for the output voltage and frequency against the variations in Z_L , u or C , under the same operating conditions of the previous techniques. The changes of V_o and F versus Z_L are demonstrated in Figure 10(a), the variation of V_o and F versus u is shown in Figures 10(b) and 10(c) presents the behavior of V_o and F against C . It can be observed that GA succeeded in finding the optimum unknown values for the whole considered range of variations in Z_L , u and C parameters. The high accuracy in the results obtained for the unknowns can be clearly realized in the smoothness of V_o and F curves.

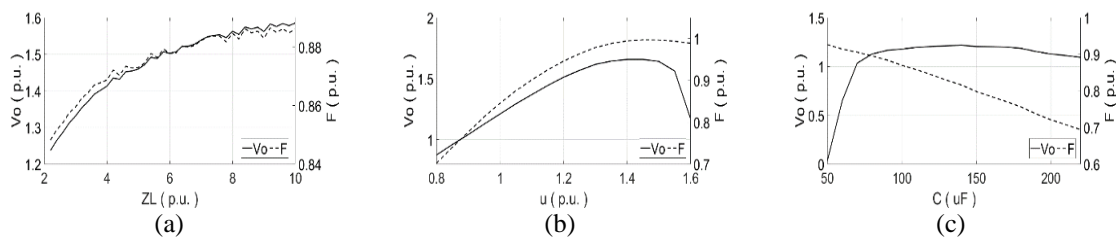


Figure 9. The results of WOA algorithm for the obtained voltage and frequency against the load, speed or the excitation capacitance (a) V_o and F versus Z_L , (b) V_o and F versus u , and (c) V_o and F versus C

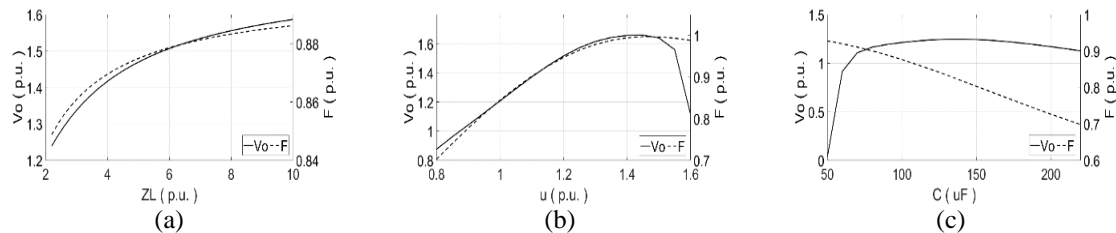


Figure 10. The results of GA for the voltage and frequency against the load, speed or the excitation capacitance (a) V_o and F versus Z_L , (b) V_o and F versus u , and (c) V_o and F versus C

The GA results for the generator's output power (P_{out}) and efficiency (η) versus the changes in Z_L , u and C parameters are shown in Figure 11. The variations of P_{out} and η versus Z_L is presents in Figure 11(a), the behavior of P_{out} and η against u is demonstrated in Figure 11(b) and the changes of P_{out} and η with C is shown in Figure 11(c). It can be seen that the shape of the obtained curves for P_{out} and η is smooth since GA approach has the ability to find the unknown parameters with high accuracy for the whole range of changes in the load, rotational speed or excitation capacitance. It is important to realize that the best output power and efficiency of the SEIG are not necessarily achieved by keep increasing the speed or the excitation capacitance. However, certain operating conditions based on optimum Z_L , u , and C values can lead to the highest possible P_{out} and η values.

Based on the comparison made between GA results with the corresponding results of each other optimization technique, it can be observed that GA is the most powerful optimization approach in finding the optimum values of unknown variables under wide range of variations in SEIG parameters. Therefore, it can be strongly recommending utilizing GA algorithm for steady state (SS) analysis of SEIG under different operating conditions. The next candidate algorithm for SS analysis of SEIG is GWO algorithm. The other five approaches (PSO, *fmincon*, *fminimax*, *fminunc*, and WOA) have failed to find accurate results for the unknown parameters under certain speed, load or excitation capacitance. Therefore, it is not recommended to utilize these five algorithms for SS analysis of SEIG, especially for wide ranges of variations in Z_L , u , or C parameters.

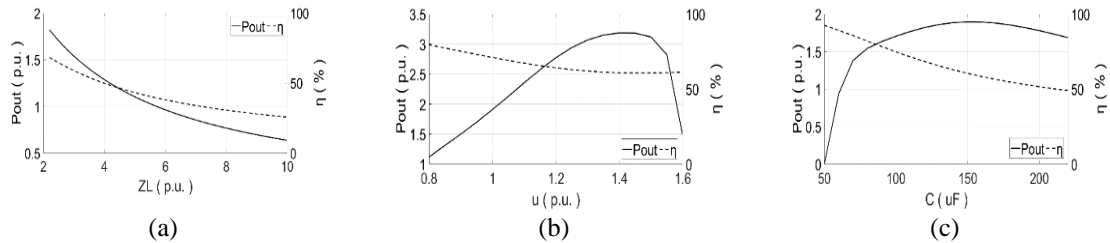


Figure 11. The results of GA for the efficiency (η) and output power (P_{out}) against the load, speed or the excitation capacitance (a) P_{out} and η versus Z_L , (b) P_{out} and η versus u , (c) P_{out} and η versus C

5. CONCLUSION

The seven optimization approaches PSO, GWO, *fmincon*, *fminimax*, *fminunc*, WOA and GA have been applied to predict the steady state performance of three-phase SEIG under the changes in rotational speed, excitation capacitance and load. Based on the results obtained, it can be concluded that the optimization approach which has the ability to find the most accurate solution for the unknown parameters is GA followed by GWO algorithm. This can be realized in the results representing the behavior of the voltage, frequency under the wide range of changes in the generator parameters.




REFERENCES

- [1] A. Rani and G. Shankar, "Standalone operation of wind turbine operated self excited induction generator," in *2016 3rd International Conference on Recent Advances in Information Technology (RAIT)*, Mar. 2016, pp. 321–325, doi: 10.1109/RAIT.2016.7507924.
- [2] M. Bašić, D. Vukadinović, I. Grgić, and M. Bubalo, "Energy efficient control of a stand-alone wind energy conversion system with AC current harmonics compensation," *Control Engineering Practice*, vol. 93, Dec. 2019, doi: 10.1016/j.conengprac.2019.104185.
- [3] S. M. Alghuwainem, "Steady-state analysis of an isolated self-excited induction generator driven by regulated and unregulated turbine," *IEEE Transactions on Energy Conversion*, vol. 14, no. 3, pp. 718–723, 1999, doi: 10.1109/60.790941.
- [4] K. A. Nigim, M. M. A. Salama, and M. Kazerani, "Identifying machine parameters influencing the operation of the self-excited induction generator," *Electric Power Systems Research*, vol. 69, no. 2–3, pp. 123–128, May 2004, doi: 10.1016/j.epsr.2003.08.003.
- [5] S. Singaravelu and S. Velusami, "Capacitive VAR requirements for wind driven self-excited induction generators," *Energy Conversion and Management*, vol. 48, no. 4, pp. 1367–1382, Apr. 2007, doi: 10.1016/j.enconman.2006.05.024.
- [6] S. N. Mahato, S. P. Singh, and M. P. Sharma, "Excitation capacitance required for self excited single phase induction generator using three phase machine," *Energy Conversion and Management*, vol. 49, no. 5, pp. 1126–1133, May 2008, doi: 10.1016/j.enconman.2007.09.007.
- [7] M. H. Haque, "Comparison of steady state characteristics of shunt, short-shunt and long-shunt induction generators," *Electric Power Systems Research*, vol. 79, no. 10, pp. 1446–1453, Oct. 2009, doi: 10.1016/j.epsr.2009.04.017.
- [8] A. Kheldoun, L. Refoufi, and D. E. Khodja, "Analysis of the self-excited induction generator steady state performance using a new efficient algorithm," *Electric Power Systems Research*, vol. 86, pp. 61–67, May 2012, doi: 10.1016/j.epsr.2011.12.003.
- [9] H. M. Hasanien and G. M. Hashem, "A cuckoo search algorithm optimizer for steady-state analysis of self-excited induction generator," *Ain Shams Engineering Journal*, vol. 9, no. 4, pp. 2549–2555, Dec. 2018, doi: 10.1016/j.asej.2017.07.003.
- [10] S. Boora, S. K. Agarwal, and K. S. Sandhu, "Optimization based performance evaluation of CEIG for rural sites," *Procedia Computer Science*, vol. 132, pp. 849–862, 2018, doi: 10.1016/j.procs.2018.05.097.
- [11] S. K. Saha and K. S. Sandhu, "Optimization techniques for the analysis of self-excited induction generator," *Procedia Computer Science*, vol. 125, pp. 405–411, 2018, doi: 10.1016/j.procs.2017.12.053.
- [12] P. C. Krause, O. Wasyuczuk, and S. D. Sudhoff, *Analysis of electric machinery and drive systems*, 2nd edition. Wiley-IEEE Press, 2002.
- [13] V. R. Sahu, R. Kesarwani, V. P. Chandran, S. Pandey, V. Kumar, and S. Vadhera, "Steady state analysis of standalone SEIG for different operating conditions with interactive MATLAB Graphical User Interface," in *2012 International Conference on Emerging Trends in Electrical Engineering and Energy Management (ICETEEEM)*, Dec. 2012, pp. 210–215, doi: 10.1109/ICETEEEM.2012.6494476.
- [14] Y. Chaturvedi, S. Kumar, and V. Gupta, "Capacitance requirement for rated current and rated voltage operation of SEIG using whale optimization algorithm," *Procedia Computer Science*, vol. 167, pp. 2581–2589, 2020, doi: 10.1016/j.procs.2020.03.315.
- [15] C.-C. Tseng, J.-G. Hsieh, and J.-H. Jeng, "Active contour model via multi-population particle swarm optimization," *Expert Systems with Applications*, vol. 36, no. 3, pp. 5348–5352, Apr. 2009, doi: 10.1016/j.eswa.2008.06.114.
- [16] M. A. Zedini, R. Pusca, A. Sakly, and M. F. Mimouni, "PSO-based MPPT control of wind-driven self-excited induction generator for pumping system," *Renewable Energy*, vol. 95, pp. 162–177, Sep. 2016, doi: 10.1016/j.renene.2016.04.008.
- [17] S. Khunkitti, N. R. Watson, R. Chatthaworn, S. Premrudeepracharn, and A. Siritaratwatt, "An improved DA-PSO optimization approach for unit commitment problem," *Energies*, vol. 12, no. 12, Jun. 2019, doi: 10.3390/en12122335.
- [18] S. Alam, G. Dobbie, Y. S. Koh, P. Riddle, and S. Ur Rehman, "Research on particle swarm optimization based clustering: A systematic review of literature and techniques," *Swarm and Evolutionary Computation*, vol. 17, pp. 1–13, Aug. 2014, doi: 10.1016/j.swevo.2014.02.001.
- [19] S. Alam, G. Dobbie, and S. U. Rehman, "Analysis of particle swarm optimization based hierarchical data clustering approaches," *Swarm and Evolutionary Computation*, vol. 25, pp. 36–51, Dec. 2015, doi: 10.1016/j.swevo.2015.10.003.
- [20] A. Naserbegi, M. Aghaie, and A. Zolfaghari, "Implementation of grey wolf optimization (GWO) algorithm to multi-objective loading pattern optimization of a PWR reactor," *Annals of Nuclear Energy*, vol. 148, Dec. 2020, doi: 10.1016/j.anucene.2020.107703.




- [21] C. Muro, R. Escobedo, L. Spector, and R. P. Coppinger, "Wolf-pack (Canis lupus) hunting strategies emerge from simple rules in computational simulations," *Behavioural Processes*, vol. 88, no. 3, pp. 192–197, Nov. 2011, doi: 10.1016/j.beproc.2011.09.006.
- [22] S. Mirjalili, "How effective is the Grey Wolf optimizer in training multi-layer perceptrons," *Applied Intelligence*, vol. 43, no. 1, pp. 150–161, Jul. 2015, doi: 10.1007/s10489-014-0645-7.
- [23] M. Premkumar, R. Sowmya, S. Umashankar, and P. Jangir, "Extraction of uncertain parameters of single-diode photovoltaic module using hybrid particle swarm optimization and grey wolf optimization algorithm," *Materials Today: Proceedings*, vol. 46, pp. 5315–5321, 2021, doi: 10.1016/j.matpr.2020.08.784.
- [24] L. S. Matott, K. Leung, and J. Sim, "Application of MATLAB and Python optimizers to two case studies involving groundwater flow and contaminant transport modeling," *Computers and Geosciences*, vol. 37, no. 11, pp. 1894–1899, Nov. 2011, doi: 10.1016/j.cageo.2011.03.017.
- [25] T. F. Coleman and Y. Li, "An interior trust region approach for nonlinear minimization subject to bounds," *SIAM Journal on Optimization*, vol. 6, no. 2, pp. 418–445, May 1996, doi: 10.1137/0806023.
- [26] M. Adeel, A. K. Hassan, H. A. Sher, and A. F. Murtaza, "A grade point average assessment of analytical and numerical methods for parameter extraction of a practical PV device," *Renewable and Sustainable Energy Reviews*, vol. 142, May 2021, doi: 10.1016/j.rser.2021.110826.
- [27] J. A. Goldbogen, A. S. Friedlaender, J. Calambokidis, M. F. McKenna, M. Simon, and D. P. Nowacek, "Integrative approaches to the study of baleen whale diving behavior, feeding performance, and foraging ecology," *BioScience*, vol. 63, no. 2, pp. 90–100, Feb. 2013, doi: 10.1525/bio.2013.63.2.5.
- [28] S. Mirjalili and A. Lewis, "The whale optimization algorithm," *Advances in Engineering Software*, vol. 95, pp. 51–67, May 2016, doi: 10.1016/j.advengsoft.2016.01.008.
- [29] Y. N. Anagreh and I. S. Al-Kofahi, "Genetic algorithm-based performance analysis of self-excited induction generator," *International Journal of Modelling and Simulation*, vol. 26, no. 2, pp. 175–179, Jan. 2006, doi: 10.1080/02286203.2006.11442366.

BIOGRAPHIES OF AUTHORS






Ibrahim Athamnah    received the B.Sc. degree in Electrical Engineering from University of Jordan, Jordan, in 1990 and the M.Sc. degree in Electrical Power Engineering from Hijjawi Faculty for Engineering Technology, Yarmouk University, Jordan, in 2022. Currently, he is seeking for enrolling a Ph.D. program in renewable energy. His research interests include renewable energy, hydrogen storage system, power generation, power electronics, MPPT controller, power grids, power supply quality, power system stability, load flow control, optimization algorithms, and artificial neural network. He can be contacted at email: ibfnae@gmail.com.



Yaser Anagreh    is a professor in Electrical Power Engineering Department at Yarmouk University, Irbid, Jordan. He received his B.Sc. in Electrical Engineering from University of Technology, Baghdad, Iraq, in 1984; M.Phil. and Ph.D. degrees in Electrical Engineering from University of Wales, Swansea, UK in 1995 and 1998, respectively. He has been a professor in YU, Irbid, Jordan since 2013. He is currently a faculty member in the Electrical Power Engineering Department at Yarmouk University. His research interests include electrical machines, electric motor drives and renewable energy systems. He can be contacted at email: anagreh@yu.edu.jo.



Aysha Anagreh    has received her B.Sc. degree in Civil Engineering/Construction Management from Yarmouk University, Irbid, Jordan in 2018 and her M.Sc. degree from Budapest University of Technology and Economics, Budapest, Hungary in 2019. She was working as a part time lecturer at both Yarmouk University and Al-Balqa' Applied University, Irbid, Jordan. She is currently applying to several US universities to pursue her Ph.D. study. Her research interests include structural engineering, construction materials, engineering education and algorithms-based engineering schemes. She can be contacted at email: aysha_yaser@yahoo.co.